PAPER

# Distinguishing carriers' and lattice temperatures through photoluminescence analysis

IOP Publishing Journal of Physics: Condensed Matter
J. Phys.: Condens. Matter **37** (2025) 435702 (7pp) https://doi.org/10.1088/1361-648X/ae1178

# Distinguishing carriers' and lattice temperatures through photoluminescence analysis

**Thomas Vezin[1], Xiangyu Zhu[2], Chloe Salhani[2,3], Marc Bescond[2,3,4], Kazuhiko Hirakawa[2] and Daniel Suchet[1,*]**

[1] Institut Photovoltaique d'Ile de France, UMR-IPVF 9006, CNRS, Ecole Polytechnique IPP, ENSCP PSL, Palaiseau, France
[2] Institute of Industrial Science, University of Tokyo, 4-6-1 Komaba, Meguro-ku, Tokyo 153-8505, Japan
[3] LIMMS/CNRS-IIS, 4-6-1 Komaba, Meguro-ku, Tokyo 153-8505, Japan
[4] Faculté des Sciences de Saint Jérôme, IM2NP, UMR CNRS 7334, Aix-Marseille Université, Case 142, 13397 Marseille Cedex 20, France

E-mail: daniel.suchet@polytechnique.edu

Received 2 June 2025, revised 5 October 2025
Accepted for publication 9 October 2025
Published 31 October 2025

**Abstract**

We report the direct and independent measurement of the lattice and the electrons temperatures in a nanocooler device (asymmetric double-barrier semiconductor heterostructure) at different operating points. Both temperatures are estimated from photoluminescence (PL) measurements—the former through the shift of the absorptance profile, the latter through the shape of the blackbody baseline. The device's cooling feature results from the thermionic extraction of electrons injected in a quantum well through an energy selective barrier. While electrons exhibit a spectacular cooling for resonant injection, the lattice temperature remains essentially unaffected, with a temperature decrease at the resolution limit. Further from resonance, both systems show an identical thermal behavior governed by Joule's heating. The similarities and discrepancies of the temperature profiles illustrate the complex thermal behavior of the system, epitomize the need of reliable thermometry method and showcase the ability of PL to do so.

Keywords: photoluminescence, temperature, hot carriers, lattice, cooling

## 1. Introduction

Thermal machines always feature a temperature difference between several parts of the system, either as a mean to convert heat into work (heat engine) or as a target of its own (heat pump, cooler). In the context of electronic devices, such a temperature difference can take place between charge carriers and their surrounding lattice; or between the device itself and its environment. In hot-carrier solar cells, the increased temperature of photogenerated electrons and holes as compared to that of the lattice allows a significant enhancement of the photovoltaic power conversion efficiency [1]. A similar temperature imbalance has been considered in metallic nano absorbers to enable strong catalytic properties [2, 3]. Conversely, thermionic cooling aims at reducing the temperature of the device by extracting energy from the carriers [4].

To evaluate the potential and understand the performance of such devices, it is crucial to have reliable estimations of temperatures. Optical thermometry has proven to be a power technique to do so. For semiconductor devices, this method consists in performing a spectral analysis of the photoluminescence (PL) signal emitted by the sample under scrutiny, providing a contactless access to the optical properties of the

* Author to whom any correspondence should be addressed.

absorber [5] and to the thermodynamic properties of the electronic populations [6].

It is however very challenging to measure simultaneously the temperature of each part of the system and assumptions are often made to deduce the temperature distributions from partial measurements. In the context of hot carrier solar cells, it is typically assumed that the lattice remains at ambient temperature while electrons and holes share the same out of equilibrium temperature [7, 8]. In the context of thermionic cooling, the lattice and the charge carriers are assumed to have the same temperature, colder than ambient.

In this work, we perform a direct and independent measurement of the lattice and carriers temperatures in a single quantum well nano-cooler. This device and its operation have been discussed elsewhere [9, 10] ; this paper focuses on the dual-thermometry. The temperature of the lattice is estimated from variation of the absorber's absorption coefficient (section 2.2.1), while the temperature of the carriers is given by the blackbody baseline of the emitted radiation (section 2.2.2). We observe that the lattice and the carriers' temperatures both depend on voltage, but exhibit different behaviors. This analysis highlights that such system may operate far from thermal equilibrium and illustrates the importance of validating the usual assumptions when assessing their performance.

## 2. Method

### 2.1. Single quantum well nanocooler

The sample analyzed is a GaAs single quantum well in an AlGaAs asymmetric double barrier, as theoretically studied in [9] and shown in figure 1. The sample is grown by molecular beam epitaxy on a n-GaAs substrate. First, 300 nm of n-GaAs is grown (Si doping density : $10^{18}\,\mathrm{cm}^{-3}$) as emitter. Then, a 5 nm undoped GaAs spacer layer is grown, before a 6 nm $Al_{0.5}Ga_{0.5}As$ barrier. The quantum well is located after this first barrier, and consists in a 6 nm thick layer of undoped GaAs. The second barrier is then grown as an undoped, 100 nm layer of $Al_{0.25}Ga_{0.75}As$. Finally, a collector layer (200 nm of n-GaAs, Si doping density : $10^{18}\,\mathrm{cm}^{-3}$) is added.

The wafer is then photolithographically patterned into mesa structures with various areas, ranging from $80\times80$ to $800\times800$ $\mu\mathrm{m}^{-2}$. (Au,Ge)Ni/Au contacts are deposited on the front and back sides of the mesas. The samples are finally annealed at 450 °C under and ambient Ar atmosphere for 5 s.

Under direct electrical polarization, carriers are resonantly injected through the first barrier from the emitter to a low energy confined state in the quantum well. Thermionic emission over the second barrier removes selectively high energy carriers from the electronic distribution, leading to the evaporative cooling of the population remaining in the well [11], and possibly of the lattice itself. In similar structures, a carrier temperature decrease of several dozens of Kelvins has been reported [12].

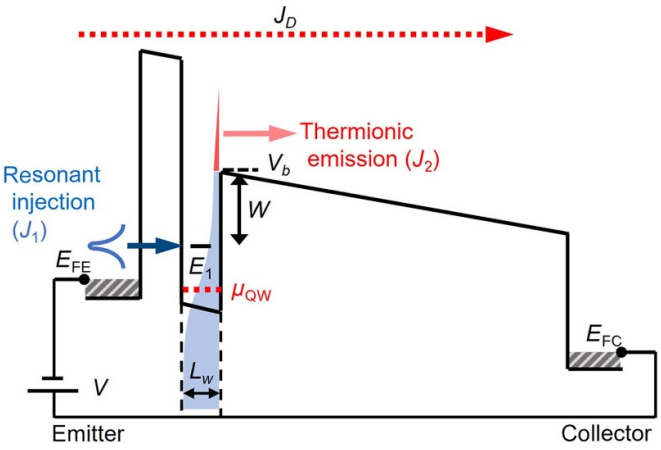


**Figure 1.** The investigated structure is the nanocooler described in [10]. An electronic current $J_1$ is resonantly injected through the first barrier in the quantum well. From there, thermionic emission above the second barrier forms a current $J_2$ which removes high energy electrons from the distribution, reducing the temperature of the remaining carriers. A non-resonant current $J_D$ above the first barrier also contributes to the system's electronic response, with an adverse heating effect. A window is opened in the collector to allow for optical characterizations. Reprinted (figure) with permission from [9], Copyright (2021) by the American Physical Society.

### 2.2. PL analysis

The measurement of both lattice and carrier temperatures relies on low intensity PL. The sample is illuminated with a continuous laser which generates electron hole pairs. As we operate in steady state, fast processes such as carrier thermalization are adiabatically eliminated and the system is measured at quasi-equilibrium. The light induced carriers are thus at thermal equilibrium with the pre existing populations. Upon recombination, they emit a radiation which follows the Generalized Planck Law [13]:

$$\phi_{\mathrm{PL}}(h\nu) = A(h\nu) \times \frac{1}{4\pi^2\hbar^3c^2} \frac{(h\nu)^2}{e^{\frac{h\nu-\Delta\mu}{k_B T_c}} - 1} \qquad (1)$$

where $A$ is the absorptance of the system, $T_c$ is the temperature of the electronic distribution and $\Delta\mu$ is the quasi Fermi level splitting between electrons in the conduction band and holes in the valence band. In the following, we will consider $\Delta\mu$ to be small enough and the energy gap to be large enough for the $-1$ term in the denominator to be negligible.The PL emission then resembles that of a thermal radiation at the carriers temperature (blackbody baseline), modulated by the absorptance profile and amplified by the QFLS.

The PL signal of the sample is acquired at ambient temperature as the device is submitted to different polarization biases, ranging from $-2$ V to $+3$ V (see figure 2). We used a blue CW laser at a wavelength of 488 nm for excitation in confocal configuration with magnification x20 (LabRAM series Raman microscope from Horiba). The laser wavelength needs to be small enough so that it can be easily filtered and removed

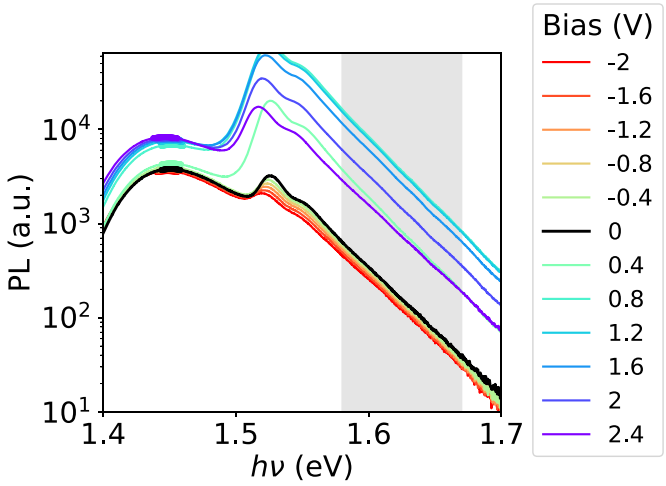


**Figure 2.** Photoluminescence (PL) spectra acquired under different polarization. The temperature of the crystal lattice is estimated from absorptance profile through the position of the bulk PL peak (bold line around 1.45 eV, see section 2.2.1). The temperature of charge carriers in the quantum well is estimated from the blackbody baseline through the slope of the high energy tail (shaded region between 1.58 eV and 1.67 eV, see section 2.2.2).

from the PL signal. However, high energy photons may cause a light-induced heating of the carriers. To prevent this parasitic effect, we used a low laser power (0.1 mW) distributed on a large spot size (20 $\mu$m), an intensity much below typical values where light induced hot carriers have been reported [14]. To confirm that the laser heating has a negligible influence on the measured temperature, we checked that the temperature measurements were unaffected by a small variation of the laser power.

Overall, the spectra show the superposition of two main contributions. Around 1.45 eV, a first PL peak results from the bulk GaAs emission. Around 1.53 eV, a second signal originates from recombination in the quantum well. The shape of the PL signal is qualitatively compatible with the profile expected from the Generalized Planck's Law equation (1), which confirms that the carriers' population follows indeed a thermal distribution with a well defined temperature. In the following, we show how the former can be used to evaluate the lattice temperature, while the latter provides access to the carrier temperature in the QW.

*2.2.1. Estimation of the lattice temperature.* The strategy to estimate the lattice temperature consists in monitoring the spectral shift of the bulk PL peak. Indeed, the position of the PL peak depends on the absorptance profile $A(h\nu)$, which depends on the absorption coefficient of the emitting material $\alpha(h\nu)$, which changes on the material's bandgap, which in turn varies with the lattice temperature. Several relations have been successfully developed to account for this variation, the most celebrated certainly being the empirical law proposed by Varshni [15–17]

$$E_g(T_L) = E_0 - a\frac{T_L^2}{T_L + b} \tag{2}$$

where $T_L$ is the lattice temperature, $a$ and $b$ are material dependent phenomenological coefficients.

Without any assumption on the actual relation between the temperature and the absorption coefficient, we perform a calibration of our temperature measurement. To do so, we place a reference sample in a cryostat and performed low illumination PL measurement. For each temperature, the position of the bulk PL peak is estimated by a quadratic fit around the maximum value. The peak shift scales linearly with the temperature with a slope of $-0.465\,\mathrm{meV.K^{-1}}$, as shown in figure 3.

This observed linear relationship is compatible with a simple interpretation. For an emission close to the material's energy gap (low absorption coefficient, leading to $A(h\nu) \propto \alpha(h\nu)$), within the parabolic band approximation (leading to $\alpha(h\nu) \propto \sqrt{h\nu - E_g(T_L)}$ [18]) and at low injection regime (as mentioned above), the Generalized Planck Law equation (1) predicts that the PL peak position is given by $\sim E_g(T_L) + k_B T_c/2$. The experiment takes place around room temperature and the Varshni's law equation (2) simplifies to a linear relation at high enough temperatures $E_g \simeq E_0 - a\,T_L$. In the calibration condition, the lattice and the carriers are both at the cryostat temperature and eventually the position of the PL peak should shift from its value $T_{ref} = 300\,\mathrm{K}$ by an amount

$$\Delta(T) = \left(\frac{k_B}{2} - a\right)(T - T_{ref}). \tag{3}$$

To evaluate the bulk temperature of the sample, we therefore estimate the position of the bulk PL peak by fitting a parabolic function, compute the shift as compared to the 0 V situation where the temperature is known to be the ambient temperature, and apply the calibrated linear relation between the peak shift and the lattice temperature. To estimate the uncertainty of the measurement, we estimate the spectral range where the amplitude of the parabolic fit remains within the experimental noise. With a typical signal-to-noise ratio of around 400 around the bulk PL peak, this spectral interval spans only on 5 meV. Considering that the location of the peak cannot be well resolved within this range, we compute the temperatures corresponding to the boundaries of this interval, and use them as lower and higher bond for the bulk temperature. This treatment leads to typical error bars of $\pm$ 5 K, which gives an estimation of the accuracy of the method.

The quantum cooler sample used in this study is mounted on a chip to facilitate the electrical connection. It has therefore a limited exchange surface with the cryostat, and a poor thermal contact. To perform the calibration, we used instead a GaAs sample and assumed that the temperature variation of the gap to be identical for both samples, despite their different doping. Furthermore, the contribution of the carriers' temperature to the PL peak shift ($\propto k_B/2$) is ten times smaller than that induced by the gap variation ($\propto a$). Considering that

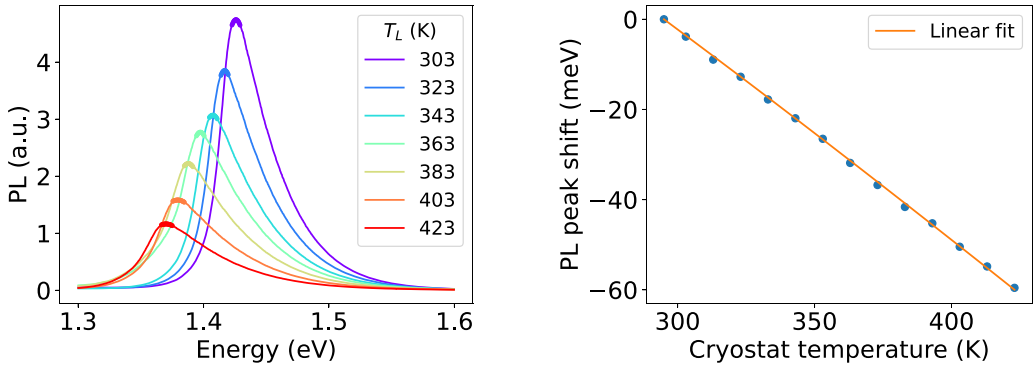


**Figure 3.** Left: PL spectra of the reference bulk sample under low illumination in a cryostat. The position of the PL peak is estimated by fitting the maximum of the curve with a quadratic function (highlighted in bold). Right: This position is reported as a function of the cryostat temperature. A linear fit shows a simple relation between the PL peak shift $\Delta E$ and the temperature change $\Delta T$ as $\Delta E[\mathrm{meV}] = -0.465\,\Delta T[\mathrm{K}]$.

the temperature differences between the lattice and the carriers remain small, we neglect this contribution—our estimation thus underestimate the temperature excursion of the lattice.

*2.2.2. Estimation of the carriers temperature.* Our strategy to estimate the carriers' temperature in the quantum well consists in comparing the exponential decay of the high energy tail of the PL spectrum. To do so, we divide the spectrum under scrutiny by a reference spectrum acquired at equilibrium ; this method is thus referred to as the 'PL ratio' method. We provide here the main lines to this method, and refer to the literature for a detailed comparison with other methods [19, 20].

According to the spectral distribution equation (1), the PL signal (divided by $(h\nu)^2$) should decay exponentially at high energy with a typical energy scale of $k_\mathrm{B}T_\mathrm{c}$. However, the absorptance profile may modulate the signal and introduce significant errors in the temperature estimation.

To circumvent this issue, it is useful to consider the ratio of the PL spectrum (PLR) under scrutiny and a reference spectrum acquired at a known temperature

$$\frac{\phi_\mathrm{PL}(h\nu)}{\phi_\mathrm{PL}^\mathrm{ref}(h\nu)} = \mathrm{cst} \times \frac{A(h\nu)}{A^\mathrm{ref}(h\nu)} \times \exp\left(\frac{h\nu}{k_\mathrm{B}T^\mathrm{ref}} - \frac{h\nu}{k_\mathrm{B}T}\right) \qquad (4)$$

Assuming that the absorptance profile over a certain range of energy remains unaffected by the electrical bias, the temperature difference between the situation under scrutiny and the reference can be obtained from a linear fit of this ratio in log scale. We emphasize that this method does not require the absorptance profile to be flat (ie $A(h\nu) = \mathrm{cst}$), but that the absorptance is the same as in the reference spectrum (ie $A(h\nu) = A^\mathrm{ref}(h\nu)$). An example for a selection of spectra is shown in figure 4. In the fitted region (shaded area), the ratio of spectra is almost flat, and well fitted with a straight line. Note that at ratio shows significant oscillations at lower energy. This feature is a signature of a variation in the absorptance due to lattice heating, which reduces the materials bandgaps. However, such mild lattice heating ($< 10\,\mathrm{K}$) should have little to no effect on the absorptance at higher energies, and in particular in the range where we fit the PLR. Error bars on the temperature measurement are estimated as the standard deviation of the values obtained by varying the boundaries of the fitted window by $\pm 20\,\mathrm{meV}$.

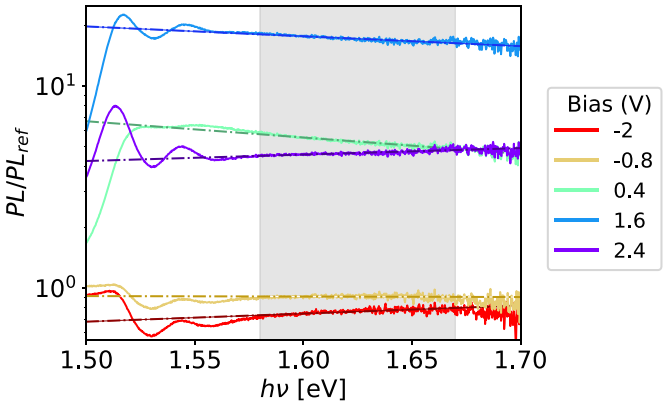


**Figure 4.** Solid lines: PL spectra at selected bias divided by the reference spectrum acquired at 0 V. Dashed lines: linear fit in log scale of the PL ratio adjusted in the high energy tail (shaded region, identical to that of figure 2). The temperature difference between the spectrum under scrutiny and that of the reference spectrum can be estimated from the slope of this line, as shown in equation (4).

## 3. Results and discussion

The temperatures of both the carriers and the lattice as estimated with the previous methods are reported in figure 5.

The most salient feature is the resonant cooling of carriers in the quantum well, as previously reported and modeled in a similar structure [10, 12]. This cooling occurs as carriers are injected from the emitter into the well, then selectively removed at high energy through thermo-ionic emission, resulting in a decrease of the average energy per carrier remaining in the well.

As the positive applied bias increases, the structure polarization brings the confined level below the bottom of the conduction band, preventing resonant injection. Furthermore, the non

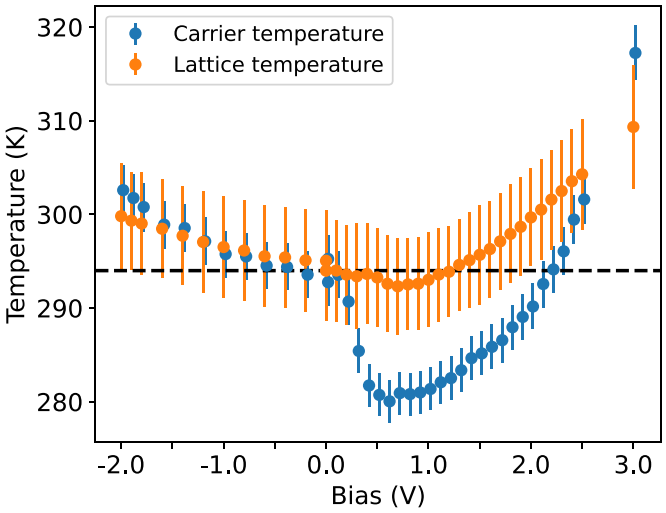


**Figure 5.** Temperature of the lattice (orange) and of the electrons in the quantum well (blue) as a function of the applied bias. The dotted line indicates room temperature at 294 K. Methods to estimate the temperatures and their uncertainties are described in the text. Several regimes can be observed, where the two systems can have very similar or significantly different temperatures, highlighting the limited validity range of usual assumptions.

resonant injection of electrons over the first barrier becomes more and more significant, and counterbalance the cooling effect through Joule's heating. As the voltage increases, this heating outweighs the cooling and the electronic distribution becomes hotter than the ambient temperature. Under negative polarization, the electrons exhibit monotonous increase in temperature with the amplitude of the applied bias.

The lattice temperature shows a significant discrepancy with that of the electrons. A very slight cooling is perhaps observed at resonance but the temperature excursion is much smaller than that of the electrons, and is at the resolution limit of our thermometry method. At 0.5 V, we report a temperature difference between the electron population and the crystal lattice above 20 K. This difference, well beyond the error bars, shows the temperature inhomogeneity in the device and epitomizes the relevance of performing independent temperature measurements for the two sub-systems.

As the applied bias is increased, positively or negatively, the lattice temperature increases under the influence of Joule's heating. For negative biases, and for large positive biases, the lattice temperature matches that of electrons and the system appears to reach a thermal equilibrium as the thermionic cooling process becomes negligible.

Our results clearly show carrier cooling under resonant bias. There is, however, no significant reduction of the lattice temperature. Lattice temperature reduction should be indeed maximum when the cooling power (CP) in the QW is the largest. In a previous study, several of the authors of the present manuscript theoretically optimized the structure based on a machine learning approach [21]. It has been shown, irrespective of the selected barrier and quantum well thicknesses, that devices reach the highest CP i) around the resonance injection point (i.e. the QW level is aligned with the Fermi level of the emitter), and ii) when the energy interval between the QW level and the top of the second thick barrier is in the range of W$\sim$70–80 meV (which roughly corresponds to the absorption of two polar optical phonons in GaAs). However, even in this optimized configuration, lattice temperature reductions will be significantly smaller than the electron's one. This is due to the important difference between the heat capacitance of electrons and phonons. In order to solve this problem, one would need to increase the electron densities in the QW regions. This could be achieved by heavily doping in the order of $10^{21} - 10^{22}\,\mathrm{cm}^{-3}$ or by considering metal/semiconductor junctions. This is however far beyond the scope of the article.

## 4. Conclusion

In this work, we have demonstrated the capability of PL spectroscopy to independently assess the temperatures of charge carriers and the lattice in a single quantum well nanocooler. By analyzing both the spectral shift of the bulk PL peak and the high-energy tail of the quantum well emission, we successfully extracted the thermal behavior of the two subsystems under various electrical biases. The uncertainty over the determination of carriers' temperature is typically 5 K, while it is twice larger, around 10 K, for lattice temperature. This is because PL is intrinsically a probe of carrier distributions. It allows for indirect determination of the lattice temperature through the variation of the bandgap, but with a lower sensitivity. Note that if the emission of GaAs had been made sharper (by reducing doping for instance), the uncertainty on lattice temperature could have been reduced dramatically.

The methods presented in this work are easy to implement and could be applied to a broad diversity of systems, provided that a clear PL signal can be collected. Carriers' temperature estimation relies on fundamental properties of spontaneous emission, independently of the emitting material. Lattice temperature estimation relies on bandgap shift, which have been reported in all families of materials (e.g. Si [22], III-V [16], II-VI [23], perovskites [24, 25] ...). Combined with PL imaging (hyperspectral), these methods can provide a contact-less temperature map, which are particularly relevant to inhomogenous systems such as thermoelectric devices or to study transport processes [26]. Combined with time resolved PL (streak camera, up conversion...), they can offer an insight into the cooling dynamics, notably for hot carrier solar cells.

Our results reveal a significant cooling of the carrier population under resonant injection, in agreement with the expected evaporative cooling mechanism. In contrast, the lattice temperature remains largely unaffected under the same conditions, confirming that carriers and the lattice can reside at distinct

temperatures—especially at resonance—contrary to assumptions often made in device modeling. Beyond the resonant regime, both temperatures converge due to dominant Joule heating effects, reinforcing the need for independent thermometric approaches to accurately capture such non-equilibrium situations. This study not only validates the use of PL spectroscopy as a reliable dual-thermometry technique in nanoscale devices but also sheds light on the subtle thermal dynamics at play in quantum heterostructures.

## Data availability statement

Raw data were generated at the University of Tokyo. Derived data supporting the findings of this study are available from the corresponding author D.S. on request.

## Acknowledgment

The author are thankful to Nathan Roubinowitz and Jean François Guillemoles for their insightful comments.

## Funding

This work is supported by GELATO ANR project (Grant No. ANR-21-CE50-0017) and by the Energy4Climate Interdisciplinary Center (E4C) of IP Paris [ANR-18-EUR-0006-02]. The authors declare no conflicts of interest.

## Author contributions

Thomas Vezin 0000-0001-5611-155X
Data curation (equal), Investigation (equal), Methodology (equal), Visualization (equal), Writing – review & editing (equal)

Xiangyu Zhu
Data curation (equal), Investigation (equal), Writing – review & editing (equal)

Chloe Salhani
Investigation (supporting)

Marc Bescond 0000-0002-2293-5371
Funding acquisition (lead), Methodology (equal), Validation (equal), Writing – review & editing (equal)

Daniel Suchet 0000-0002-4034-1016
Conceptualization (equal), Formal analysis (equal), Investigation (equal), Methodology (equal), Project administration (equal), Writing – original draft (equal)

## References

[1] Ross R T and Nozik A J 1982 Efficiency of hot-carrier solar energy converters *J. Appl. Phys.* **53** 3813–8
[2] Guzelturk B *et al* 2020 Nonequilibrium thermodynamics of colloidal gold nanocrystals monitored by ultrafast electron diffraction and optical scattering microscopy *ACS Nano* **14** 4792–804
[3] Takeda Y, Sato S and Morikawa T 2022 Hot-carrier photocatalysts for artificial photosynthesis *J. Chem. Phys.* **5** 0088459
[4] Mahan G D 1994 Thermionic refrigeration *J. Appl. Phys.* **76** 4362–6
[5] Katahara J K and Hillhouse H W 2014 Quasi-Fermi level splitting and sub-bandgap absorptivity from semiconductor photoluminescence *J. Appl. Phys.* **116** 173504
[6] Shah J and Leite R C C 1969 Radiative recombination from photoexcited hot carriers in GaAs *Phys. Rev. Lett.* **22** 1304–7
[7] Dubi Y and Sivan Y 2019 "Hot" electrons in metallic nanostructures—non-thermal carriers or heating? *Light: Sci. Appl.* **8** 89
[8] Vezin T, Roubinowitz N, Lombez L, Guillemoles J-F and Suchet D 2024 Direct determination of electron and hole temperatures from continuous-wave photoluminescence measurements *Phys. Rev. B* **110** 125207
[9] Zhu X, Bescond M, Onoue T, Bastard G, Carosella F, Ferreira R, Nagai N and Hirakawa K 2021 Electron transport in double-barrier semiconductor heterostructures for thermionic cooling *Phys. Rev. Appl.* **16** 064017
[10] Bescond M, Dangoisse G, Zhu X, Salhani C and Hirakawa K 2022 Comprehensive analysis of electron evaporative cooling in double-barrier semiconductor heterostructures *Phys. Rev. Appl.* **17** 014001
[11] Suchet D, Jehl Z, Okada Y and Guillemoles J-F 2017 Influence of Hot-Carrier Extraction from a photovoltaic absorber: an evaporative approach *Phys. Rev. Appl.* **8** 034030
[12] Yangui A, Bescond M, Yan T, Nagai N and Hirakawa K 2019 Evaporative electron cooling in asymmetric double barrier semiconductor heterostructures *Nat. Commun.* **10** 4504
[13] Wurfel P 1982 The chemical potential of radiation *J. Phys. C: Solid State Phys.* **15** 3967–85
[14] Giteau M, de Moustier E, Suchet D, Esmaielpour H, Sodabanlu H, Watanabe K, Collin S, Guillemoles J-F and Okada Y 2020 Identification of surface and volume hot-carrier thermalization mechanisms in ultrathin GaAs layers *J. Appl. Phys.* **128** 193102
[15] Varshni Y 1967 Temperature dependence of the energy gap in semiconductors *Physica* **34** 149–54
[16] O'Donnell K P and Chen X 1991 Temperature dependence of semiconductor band gaps *Appl. Phys. Lett.* **58** 2924–6
[17] Pässler R 2003 Semi-empirical descriptions of temperature dependences of band gaps in semiconductors *Phys. Status Solidi b* **236** 710–28
[18] Yu P Y and Cardona M 2010 *Fundamentals of Semiconductors: Physics and Materials Properties* (Graduate Texts in Physics) (Springer)
[19] Esmaielpour H, Lombez L, Giteau M, Guillemoles J-F and Suchet D 2022 Impact of excitation energy on hot carrier properties in InGaAs multi-quantum well structure *Prog. Photovolt., Res. Appl.* **30** 1354–62
[20] Esmaielpour H, Lombez L, Giteau M, Delamarre A, Ory D, Cattoni A, Collin S, Guillemoles J-F and Suchet D 2020 Investigation of the spatial distribution of hot carriers in quantum-well structures via hyperspectral luminescence imaging *J. Appl. Phys.* **128** 165704
[21] Fernandez J G, Etesse G, Seoane N, Comesaña E, Hirakawa K, Garcia-Loureiro A and Bescond M 2024 A novel machine learning workflow to optimize cooling devices grounded in solid-state physics *Sci. Rep.* **14** 28545
[22] Bludau W, Onton A and Heinke W 1974 Temperature dependence of the band gap of silicon *J. Appl. Phys.* **45** 1846–8
[23] Fonthal G, Tirado-Mejía L, Marín-Hurtado J, Ariza-Calderón H and Mendoza-Alvarez J 2000

Temperature dependence of the band gap energy of crystalline CdTe *J. Phys. Chem. Solids* **61** 579–83
[24] Dar M I, Jacopin G, Meloni S, Mattoni A, Arora N, Boziki A, Zakeeruddin S M, Rothlisberger U and Grätzel M 2016 Origin of unusual bandgap shift and dual emission in organic-inorganic lead halide perovskites *Sci. Adv.* **2** e1601156
[25] Diroll B T, Zhou H and Schaller R D 2018 Low-temperature absorption, photoluminescence and lifetime of CsPbX3 (X = Cl, Br, I) nanocrystals *Adv. Funct. Mater.* **28** 1800945
[26] Vezin T, Esmaielpour H, Lombez L, Guillemoles J-F and Suchet D 2024 Optical determination of thermoelectric transport coefficients in a hot-carrier absorber *Phys. Rev. Appl.* **22** 034018